Application of Percolation Theory to Noncatalytic Gas-Solid Reactions

Previous models of noncatalytic gas-solid reactions are based primarily on parallel-pore representations, thus excluding important topological effects of the porous medium. This paper utilizes network representations and percolation theory to develop expressions for pore closure time and the evolution of accessible volume, effective diffusivity, and conversion rates.

Y. C. YORTSOS and M. SHARMA
Departments of Petroleum and Chemical Engineering
University of Southern California
Los Angeles, CA 90089

SCOPE

Many processes pertinent to chemical engineering operations involve the physicochemical interaction of fluids with the solid surfaces of a porous medium. A particularly broad class is characterized by the continuous-in-time reduction of the available surface area as a result of surface chemical reactions (e.g., catalyst deactivation and noncatalytic gas-solid reaction processes). This reduction is manifested by progressively lower conversion rates and invariably leads to pore closure (plugging). Previous mathematical models based on parallel-pore representations (e.g., Ramachandran and Smith, 1977; Christman and Edgar, 1983) provide a good description of the process at the local (pore) level, but are inherently inadequate for the accurate prediction of the time rate of change of accessible surface area and volume, effective diffusivity, and ultimately conversion efficiency and pore blockage time. Subsequent investigations by Gavalas (1980), and Bhatia and Perlmutter (1980), among others, imparted considerable insight into the effects of the topology of the porous medium by utilizing random pores.

In this paper we follow a somewhat different approach based on a network representation of the porous medium. By using population balances and elements from percolation theory, we develop a general theory that rigorously accounts for the effect of geometrical (e.g., pore size distribution) and topological (e.g., connectivity, accessibility) aspects of the porous structure on the evolution in time of the above quantities. The theory provides significant insight into the intricate effects of the pore structure on the performance of several such processes.

CONCLUSIONS AND SIGNIFICANCE

Application of the theory to computationally manageable networks, such as Bethe lattices, allows for a direct and computationally simple calculation of the pore closure time as well as the evolution in time of accessible surface area and volume, conversion efficiency, and effective diffusivity. The input required for the implementation of the model consists of the true pore size distribution and the coordination number of the network. Closed-form expressions derived for the most important quantities associated with noncatalytic gas-solid reactions, are directly applicable to processes globally in the kinetic control regime. A simplified mathematical formulation is also developed for processes that do not satisfy the kinetic control limitations. This formulation contains a new representation of the effective diffusivity, previously considered constant or taken to be proportional to the local porosity (Garza-Garza and Dudukovic, 1981).

For illustration purposes, the results are compared to the predictions obtained based on parallel-pore models of constant pore radius. It is shown that a proper accounting of the nonaccessible fraction of open pores leads to higher estimates of pore closure time and lower estimates of conversion as compared to parallel-pore models. This discrepancy is found to increase with an increase in the Biot number, a decrease in the coordination number of the porous network, and an increase in process time.

INTRODUCTION

Large classes of operations of engineering interest involve physicochemical interactions of a fluid with the solid surfaces of a porous medium. Several of these are characterized by a continuous alteration of the pore structure by virtue of physical changes—e.g., particle deposition in deep bed filtration (Tien and Payatakes, 1979) and fines migration in porous reservoirs (Gruesbeck

and Collins, 1982)—or chemical reactions—e.g., catalyst deactivation phenomena (Butt, 1972) and noncatalytic gas-solid reactions (Ramachandran and Doraiswamy, 1982). A particular feature common to such processes is the reduction of the surface area available for fluid-solid interaction leading to a continuous decrease of the capacity for flow, diffusion, and reaction, progressively lower rates of conversion efficiency, and ultimately to pore closure (plugging).

The mathematical description of the process performance is considerably complicated due to the continuous evolution of the pore structure as a function of time. Of the various modeling attempts that have been made in the past, the majority are based on the description of the porous media in terms of simple geometric models—e.g., parallel pores (Ramachandran and Smith, 1977; Christman and Edgar, 1983) or solid (grain) particles of spherical shape (Szekely and Evans, 1970). Although correctly emphasizing purely geometrical aspects of the porous structure such as pore size distribution, these models fail to properly account for important topological effects that govern adjacent pore interaction. Thus, despite a certain degree of success in predicting volume-related aspects of the process, such as efficiency and pore blockage time, previous models are inherently inadequate in predicting the evolution in time of topology-related aspects such as effective diffusivity (for gas diffusion) and flow permeability (for fluid flow).

Several studies conducted in the context of gasification of solids allow a more elaborate statistical representation of the pore structure (e.g., Gavalas, 1980; Bhatia and Perlmutter, 1980). However, a concrete elucidation of the important role of topology and connectivity in determining transport properties in porous media was only recently obtained in fluid flow in porous media studies associated with the enhanced recovery of oil. Using lattice and network representations, Scriven, Davis and co-workers (Larson et al., 1981a, b; Heiba et al., 1982, 1983, 1984; Mohanty et al., 1982) have successfully applied concepts from percolation theory, originating from research in physics of hetereogeneous materials (Broadbent and Hammersley, 1957; Shante and Kirkpatrick, 1971), to devise computationally simple schemes for the accurate prediction of transport properties in porous media.

The objective of this paper is to implement a similar approach, based on network representation and percolation theory, in order to develop more highly accurate mathematical models for processes that involve a continuous evolution of the pore structure. For purposes of illustration, the present investigation focuses on noncatalytic, gas-solid reactions that result in a continuous decrease of the pore size and ultimately lead to pore closure. Without loss in generality, we consider a local, representative element of the porous medium, within which the process is locally at the kinetic control regime. The results obtained can be incorporated in principle into a global, continuous model the parameters of which do not necessarily satisfy kinetic control limitations. On the other hand, if the process is globally at kinetic control, the ensuing results describe the global behavior of the process. A related application of the theory to deep-bed filtration is currently in progress (Sharma and Yortsos, 1984). Similar applications to other closely related processes, such as catalyst deactivation, appear to be readily implemented by direct extension.

MATHEMATICAL FORMULATION

Single-Pore Formulation

We consider a local element of a porous medium exposed to a reactant gas at constant local concentration, C_A. By virtue of gas diffusion through the pores of the medium and the deposited solid product, the reactant gas participates in a chemical reaction with the original solid phase according to the scheme

$$aA(g) + bB(s) \rightarrow cC(g) + dD(s) \tag{1}$$

Following previous formulation of noncatalytic gas-solid reactions using single-pore models (Shankar and Yortsos, 1983), the pore diameter r and the reaction interface r_f associated with a single-pore of original size r_o (Figure 1a), are determined in the limit of kinetic control as the solution of the dimensional equations

$$\frac{dr}{dt} = -\frac{\hat{K}}{G_s(r;r_o)} \tag{2}$$

$$r^s = \alpha + (1-\alpha) r_f^s \tag{3}$$

subject to the initial conditions.

$$r = r_o \quad ; \quad t = 0 \tag{4}$$

In the above, $\hat{K}$ is the kinetic constant

$$\hat{K} = \frac{(\alpha - 1) M_D d C_A}{(1 - \epsilon_D) r_o} K \tag{5}$$

the dimensionless parameter $\alpha > 1$ expresses the ratio in molar volumes between deposited solid product and solid reactant

$$\alpha = \frac{d}{b} \frac{V_D(1 - \epsilon_B)}{V_B(1 - \epsilon_D)} \tag{6}$$

and it has been tacitly assumed that the reaction follows first-or-

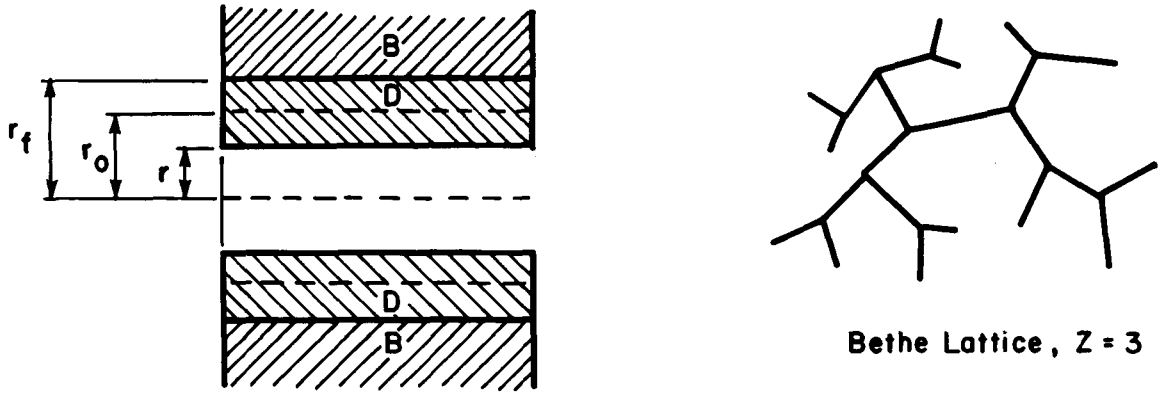

Figure 1. (a) Single pore dimensions; (b) Network representation.

der kinetics. The latter assumption, although not restrictive, is convenient for a simplified description, and can easily be relaxed whenever appropriate. The dimensionless function G_s reflects gas diffusion within the product layer and reaction at the reaction interface for two different pore geometries ($s = 1$, slab; $s = 2$, cylindrical)

$$G_s = \begin{cases} 1 + \left(\dfrac{\alpha}{\alpha - 1}\right)\dfrac{K}{D_e}(r_o - r) \quad ; \quad s = 1 \\ \left[\dfrac{\alpha - 1}{\alpha - \left(\dfrac{r}{r_o}\right)^2}\right]^{1/2} + \dfrac{Kr_o}{D_e}\ln\left[\dfrac{\alpha r_o^2 - r^2}{r^2(\alpha - 1)}\right]; s = 2 \end{cases} \tag{7}$$

Experimental determination of the kinetic (K) and diffusion (D_e) constants completes the mathematical formulation in a single pore.

Equations 2 and 4 specify a correspondence between r, r_o, and t. Integration of Eq. 2 determines the instantaneous radius r of a pore of original size r_o

$$\int_{r_o}^{r_o} G_s(r;r_o)dr = -\hat{K}t \tag{8}$$

and the associated time $t_p(r_o)$ for the closure of a pore of size r_o:

$$t_p(r_o) = \frac{1}{\hat{K}}\int_0^{r_o} G_s(r;r_o)dr \tag{9}$$

The last equation defines a one-to-one correspondence between time and original radius. In view of its monotonicity features, ($G_s > 0$), this functional relationship can be used to parametrize time in terms of a continuously increasing variable r_i

$$t = t_p(r_i) \tag{10}$$

For slab (parallel-plate) geometries ($s = 1$), Eqs. 8, 9, and 10 can be considerably simplified. After some algebraic manipulations we obtain

$$r_o - r = r_i \quad ; \quad r_o > r_i \tag{11}$$

$$t_p(r_o) = \frac{1}{\hat{K}}\left(r_o + \frac{r_o^2\alpha K}{2D_e(\alpha - 1)}\right) \tag{12}$$

$$t = t_p(r_i) \tag{13}$$

Thus, at time t, defined by Eqs. 12 and 13, corresponding to a time when a pore of original size r_i is completely blocked, pores of original size $r_o > r_i$ that are continuously reacting have radius given by Eq. 11. Similar expressions can also be obtained for cylindrical geometries. However, in view of the mathematical simplicity of Eqs. 11–13 we elect to consider parallel-plate geometries in the remaining part of this investigation. Extension to other pore geometries follows directly at the expense of somewhat lengthier calculations.

Network Formulation

Following Larson et al. (1981a), we next assume that the local porous medium element is originally represented by a three-dimensional network or lattice configuration consisting of sites (pore bodies) and bonds (pore throats) of coordination number Z (Figure 1b). For the problem in consideration we assign negligible volume to sites and postulate bonds of constant length and a uniform pore radius. An initial distribution function of pore radii, $f(r)$, that can in principle be determined experimentally, is assigned to the bonds of the network. Higher-order approximation models that allow for a distribution of pore lengths and include sites of nonnegligible volume can, of course, be similarly developed.

At any time of the process parametrized by Eq. 13, the network consists of three sets of pores:

1. Pores that have completely reacted, are blocked, and do not participate in further reaction, of fraction X_b.
2. Pores that have partially reacted, are not blocked (open), and are accessible to gas diffusion and reaction, of fraction X_a and current size distribution $f_a(r,r_i)$.
3. Pores that have partially reacted, are not blocked (open), but are inaccessible to gas diffusion and further reaction, of fraction $X_{na} = 1 - X_b - X_a$ and current size distribution $f_{na}(r,r_i)$.

All fractions are defined based on the original number of open pores. By definition, pores belonging to set 1 have original pore radius $r_o < r_i$, pores in set 2 have original pore radius $r_0 > r_i$, while pores in set 3 have original pore radius $0 < r_o < \infty$. The actual pore size distribution of each set can be calculated following the equations for the rate of pore size reduction (Eqs. 2–4).

The determination at any time t of the fractions of the three sets of pores and their actual size distribution requires a differential approach, using population balances at each calculation step Δr_i. However, the fraction of open, accessible pores, X_a, can be obtained directly by use of percolation theory as follows. At any stage r_i all pores of original size $r_o > r_i$ are allowed for occupancy by pores that have not completely reacted (become blocked). The fraction allowed for occupancy is $1 - X_i$ where

$$X_i = \int_0^{r_i} f(r)dr \tag{14}$$

The actual fraction of open pores that are accessible (set 2) is then given by the accessibility function of the network X^A, evaluated at the fraction $1 - X_i$

$$X_a = X^A(1 - X_i) \tag{15}$$

The accessibility function $X^A(p)$ can be calculated exactly for Bethe tree lattices, given the fraction of bonds allowed for occupancy p and the lattice coordination number Z (Fisher and Essam, 1961). Approximate expressions for $X^A(p)$ for other lattices are obtainable from effective medium theory (Kirkpatrick, 1973), when p is close to 1, and from scaling theory (Stauffer, 1979), when p is close to the percolation threshold, p_c. The latter denotes the minimum value in the fraction of pores allowed to be open for the existence of a nonzero fraction of accessible open pores $X^A(p)$. Previous theoretical work and extensive Monte Carlo simultations have established with considerable accuracy the following dependence of p_c on Z and the dimensionality of the lattice D

$$p_c = \begin{cases} 1 & \text{for } 1 - D \text{ lattices} \\ \dfrac{D}{(D-1)Z} & \text{for lattices of dimension } D \\ \dfrac{1}{Z-1} & \text{for Bethe trees} \end{cases} \tag{16}$$

Typical accessibility functions for a Bethe tree lattice are shown in Figure 2.

Following the above premises, the time t_p^* when reaction ceases and the local porous medium element is completely blocked is obtained from the equation

$$1 - X_i^* = p_c \tag{17}$$

which in view of Eqs. 13 and 14 occurs at the critical radius r_i^*

$$\int_{r_i^*}^{\infty} f(r)dr = p_c \tag{18}$$

$$t_p^* = t_p(r_i^*) \tag{19}$$

Quantities of interest associated with the pore structure such as conversion, accessible surface area and volume, and effective dif-

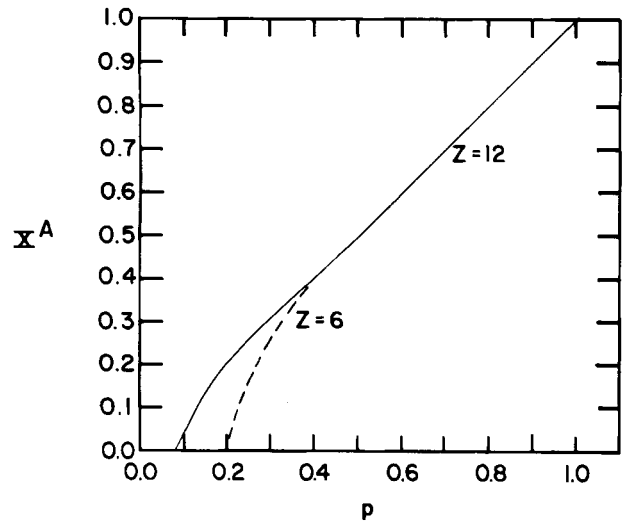

Figure 2. Typical accessibility functions for Bethe lattices.

fusivity can be calculated at any time as shown in the following sections.

Population Balances

At step Δr_i all pores belonging to set 2 of current radius $0 < r < \Delta r_i$ are blocked; thus they are transferred to set 1

$$\Delta X_b = x_a f_a(0,r_i)\Delta r_i \tag{20}$$

By virtue of connectivity, at the completion of step Δr_i some pores of set 2 become disconnected; thus they are transferred to set 3. This process is assumed to occur randomly, and therefore the pore size distribution of the differential set being removed is $f_a(r,r_i)$. The respective population balances for sets 1 and 2, and 3 can now easily be derived. We obtain in differential notation

$$\frac{\partial}{\partial r}[X_a f_a] + \frac{\partial}{\partial r}\left[X_a f_a \frac{dr}{dr_i}\right] = -\frac{dX_{na}}{dr_i} f_a \tag{21}$$

$$\frac{\partial}{\partial r_i}[X_{na} f_{na}] = \frac{dX_{na}}{dr_i} f_a \tag{22}$$

$$\frac{dX_b}{dr_i} = X_a f_a(0,r_i) \tag{23}$$

It should be noted that Eq. 23 is not linearly independent, as it can be obtained from integration of Eq. 21 and use of the relationship

$$X_a + X_{na} + X_b = 1 \tag{24}$$

We next proceed for the evaluation of $f_a(r,r_i)$. Using Eq. 11, Eq. 21 becomes

$$\frac{\partial}{\partial r_i}[X_a f_a] - \frac{\partial}{\partial r}[X_a f_a] = -\frac{dX_{na}}{dr_i} f_a \tag{25}$$

along with boundary conditions

$$f_a(r,0) = f(r) \tag{26a}$$

$$f_a(\infty,r_i) = 0 \tag{26b}$$

and the normalization condition

$$\int_0^\infty f(r,r_i)dr = 1 \tag{26c}$$

An analysis of Eqs. 25 and 26 reveals that the solution for f_a is of the separable form

$$f_a(r,r_i) = f(r + r_i)\quad \theta(r_i) \tag{27}$$

where θ is a function of r_i (Appendix). The latter can be readily obtained from Eq. 26c. We obtain

$$f_a(r,r_i) = \frac{f(r + r_i)}{1 - X_i} \tag{28}$$

In view of Eq. 28, the population balances, Eqs. 21–23, are modified to the following equations

$$\frac{dX_b}{dr_i} = \frac{X_a f(r_i)}{1 - X_i} \tag{29}$$

$$X_h f_{na} = \int_0^{r_i} \frac{dX_b f(r + r_i)}{dr_i\ (1 - X_i)} dr_i \tag{30}$$

Integration of Eq. 29 yields the fraction of pores that have completely reacted at stage r_i

$$X_b = \int_0^{X_i} \frac{X^A(1 - X_i)\ dX_i}{1 - X_i} \tag{31}$$

As anticipated, due to network accessibility the number of completely reacted pores is less than the number of completely reacted pores when all pores are accessible, X_i, in contrast to what is typically assumed in previous parallel-pore models.. (Note that $X^A(p) < p$). Typical plots of X_b vs. X_i are shown in Figure 3 for Bethe tree lattices of different coordination numbers. The evolution in time of X_b can readily be constructed by making use of Eqs. 12–14.

RESULTS

Plugging Time

The calculation of plugging time t_p^* is based on Eqs. 18 and 19. Using Eqs. 12 and 13 we obtain

$$t_p^* = \frac{1}{K}\left[r_i^* + (r_i^*)^2 \frac{\alpha K}{2D_e(\alpha - 1)}\right] \tag{32}$$

For convenience in presentation we compare t_p^* to the plugging time $\overline{t_p}$ of an idealized porous network that consists of identical

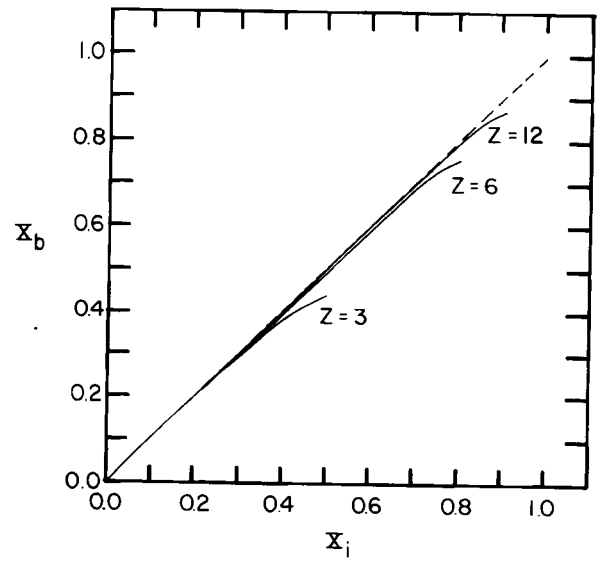

Figure 3. Fraction of completely blocked pores.

pores of original size equal to the average original pore size $\bar{r}_o$. By construction, all pores of the idealized network are accessible at any time, thus

$$\bar{t}_p = \frac{1}{\bar{K}}\left[\bar{r}_o + (\bar{r}_o)^2 \frac{\alpha K}{2D_e(\alpha - 1)}\right] \tag{33}$$

It should be noted that use of a variable pore size distribution in the parallel pore model, although feasible, would result in a plugging time obtained by Eq. 33 with the highest radius of the distribution r_{max} replacing r_o. As this time becomes infinite in the following special cases, we elected to normalize our results on the basis of a parallel-pore model of uniform original size. We next define a modified Biot number, $\overline{Bi}$, based on the average original pore size

$$\overline{Bi} = \frac{\alpha K \bar{r}_o}{D_e(\alpha - 1)} \tag{34}$$

Comparison of Eq. 32 and 33 results in the expression

$$\frac{t_p^*}{\bar{t}_p} = \frac{2\frac{r_i^*}{\bar{r}_o} + \overline{Bi}\left[\frac{r_i^*}{\bar{r}_o}\right]^2}{2 + \overline{Bi}} \tag{35}$$

For values of coordination number typical of porous media (large Z), we readily obtain $r_i^* > \bar{r}_o$. Thus Eq. 35 predicts an actual plugging time that is larger than the plugging time obtained for an always accessible porous network. The discrepancy increases with an increase in the average Biot number. This discrepancy, which is a manifestation of topology and geometry effects, is illustrated in the following special cases. We consider Poisson, Gaussian, and Rayleigh original pore size distributions:

Poisson Distribution

We have

$$f(r_o) = \mu e^{-\mu r_o}, \tag{36}$$

$$\bar{r}_o = \frac{1}{\mu}$$

Solution o Eq. 18 determines the critical radius r_i^*:

$$r_i^* = -\frac{1}{\mu} \ln p_c \tag{37}$$

Substitution of Eq. 37 into Eq. 35 results in

$$\frac{t_p^*}{\bar{t}_p} = \frac{-2\ln p_c + \overline{Bi}(\ln p_c)^2}{2 + \overline{Bi}} \tag{38}$$

The ratio in plugging times is plotted in Figure 4 as a function of Z for a Bethe tree lattice for various values of $\overline{Bi}$. For $Z > 1 + e \simeq 3.7$ the actual plugging time t_p^* is larger than $\bar{t}_p$ and increases with an increase in $\overline{Bi}$. For high coordination numbers Z, representing highly branched porous media, the actual plugging time is two- to threefold greater than the plugging time based on the average pore size.

Gaussian Distribution

We have

$$f(r_o) = \frac{\sqrt{2}}{\sqrt{\pi}\sigma}\frac{1}{\left[1 + \text{erf}\left(\frac{\mu}{\sigma\sqrt{2}}\right)\right]}\exp\left[-\frac{1}{2}\left(\frac{r_o - \mu}{\sigma}\right)^2\right] \tag{39}$$

$$\bar{r}_o = \mu$$

The critical radius r_i^* is determined from the solution of the equation

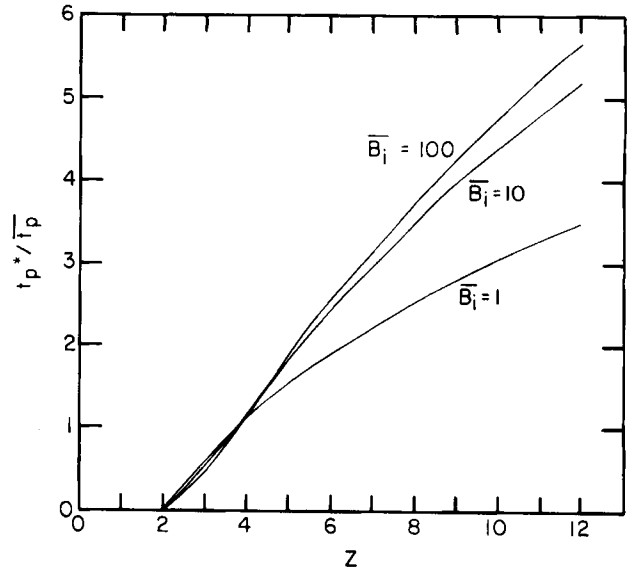

Figure 4. Ratio of plugging times for Poisson distribution.

$$\text{erf}\left[\frac{\frac{r_i^*}{\mu} - 1}{\frac{\sigma\sqrt{2}}{\mu}}\right] = 1 - p_c \tag{40}$$

For any values of p_c Eq. 40 predicts $r_i^* > \bar{r}_o$. In the limit of small values of standard deviation $\sigma \to 0$ (single size distribution) Eq. 40 yields the correct limit $r_i^* \to r_o$, $t_p^* \to \bar{t}_p$, as expected. The ratio in plugging times is plotted in Figure 5 as a function of Z for various values of $\overline{Bi}$ and the ratio σ/μ. It is evident that the deviation in estimating plugging time increases with an increase in $\overline{Bi}$ and the standard deviation σ.

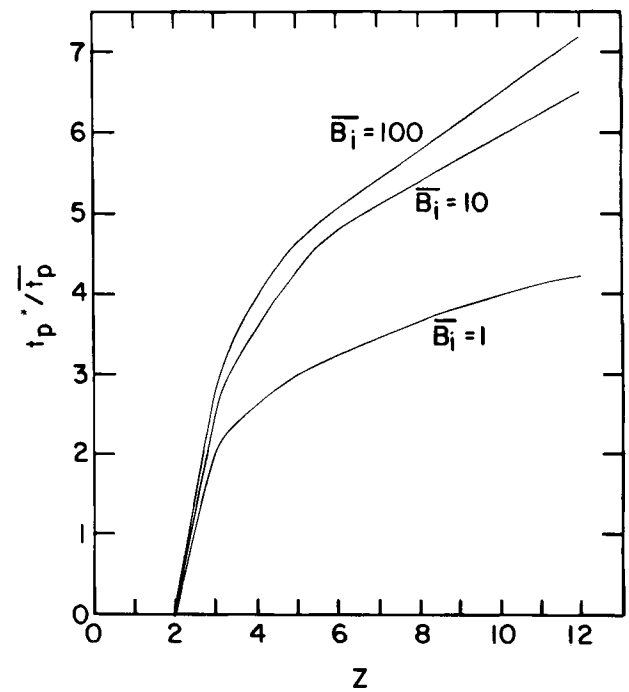

Figure 5. Ratio of plugging times for normal distribution.

Rayleigh Distribution

We consider the distribution

$$f(r_o) = \begin{cases} 0 & r_o < a \\ 2\mu(r_o - a)\exp[-\mu(r_o - a)^2] & r_o > a \end{cases} \tag{41}$$

$$\bar{r}_o = a + \frac{\sqrt{\pi}}{2\sqrt{\mu}}$$

Solution of Eq. 18 defines the critical radius r_i^*

$$\frac{r_i^*}{\bar{r}_o} = \frac{\left(1 + \left(-\frac{\ln p_c}{\mu}\right)^{1/2}\right)}{a + \frac{1}{2}\frac{\sqrt{\pi}}{\sqrt{\mu}}} \tag{42}$$

For values of $p_c < e^{-\pi/4} = 0.4559$, the deviation in the estimate of plugging time increases with an increase in Z, $\bar{Bi}$, and a decrease in the value of $a\sqrt{\mu}$ (Figure 6). Note, however, that in this case the magnitude of deviation is smaller than in previous distributions. In the limit $\mu \to \infty$ (single pore size distribution), $t_p^* \to \bar{t}_p$, as anticipated.

Conversion

At any stage during the reaction process, conversion of the solid reactant occurs on pores that are open and accessible to gas diffusion (Set 2.)

Following the preceding formulation, the set of such pores has fraction X^A and consists of pores of original radius $r_o > r_i$. At an increment of time Δt, or equivalently at an increment Δr_i, the reaction interface of such pores recedes by Δr_f. For a parallel plate (slab geometry) model we obtain from Eqs. 3 and 11

$$\Delta r_f = -(\alpha - 1)\Delta r = (\alpha - 1)\Delta r_i \tag{43}$$

The corresponding increase in conversion ΔR (in mass/original volume) from all pores belonging to this set is

$$\Delta R = C X^A(1 - X_i)\Delta r_i \tag{44}$$

where the constant C is related to the original specific surface S^0 by

$$C = \frac{S^0 \rho_\beta}{2(a-1)} \tag{45}$$

Integration of Eq. 44 results into

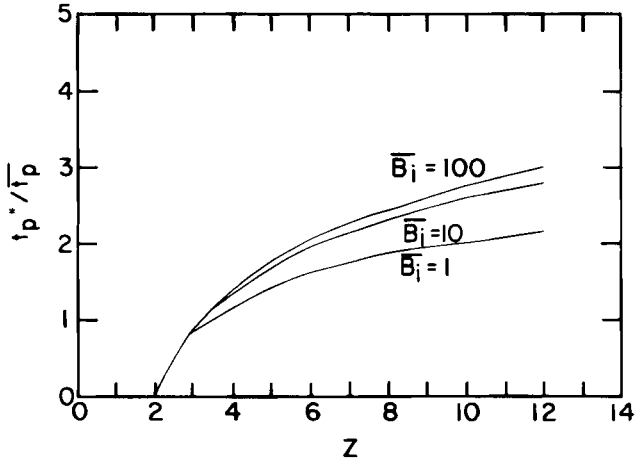

Figure 6. Ratio of plugging times for Rayleigh distribution.

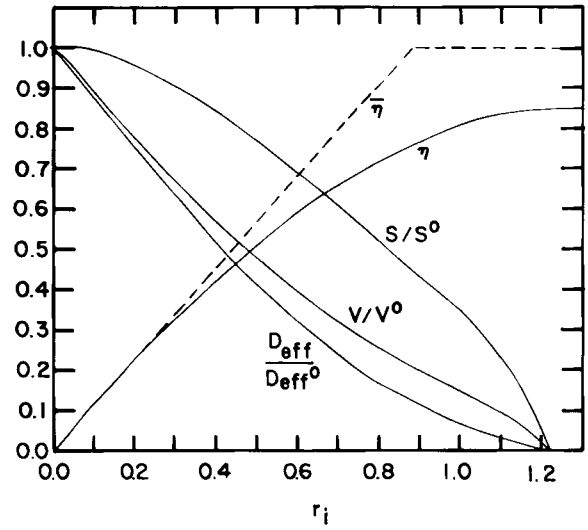

Figure 7. Normalized conversion, accessible surface area, volume, and effective difussivity for Rayleigh distribution (a = 0), Z = 6, plotted vs. r_i.

$$R = C\int_0^{r_i} X^A(1 - X_i)dr_i \tag{46}$$

For convenience we normalize conversion by the conversion $\bar{R}$ of the idealized porous network. Since all the pores of the latter are always accessible we have

$$\bar{R} = \begin{cases} Cr_i & r_i < \bar{r}_o \\ C\bar{r}_o & r_i > \bar{r}_o \end{cases} \tag{47}$$

thus

$$\eta = \frac{R}{\bar{R}} = \begin{cases} \frac{1}{r_i}\int_0^{r_i} X^A(1 - X_i)dr_i & r_i < \bar{r}_o \\ \frac{1}{\bar{r}_o}\int_0^{r_o} X^A(1 - X_i)dr_i & r_o > \bar{r}_o \end{cases} \tag{48}$$

Plotted in Figures 7–10 is the normalized conversion as a function of r_i, calculated for a porous network consisting of a Bethe tree lat-

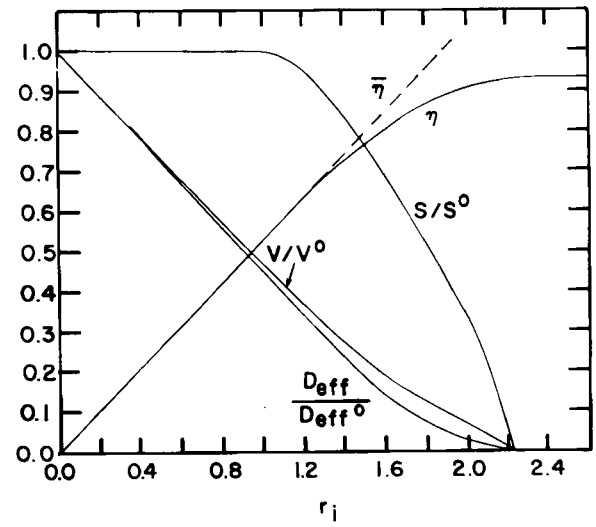

Figure 8. Normalized conversion, accessible surface area, volume, and effective difussivity for Rayleigh distribution (a = 1), Z = 6, plotted vs. r_i.

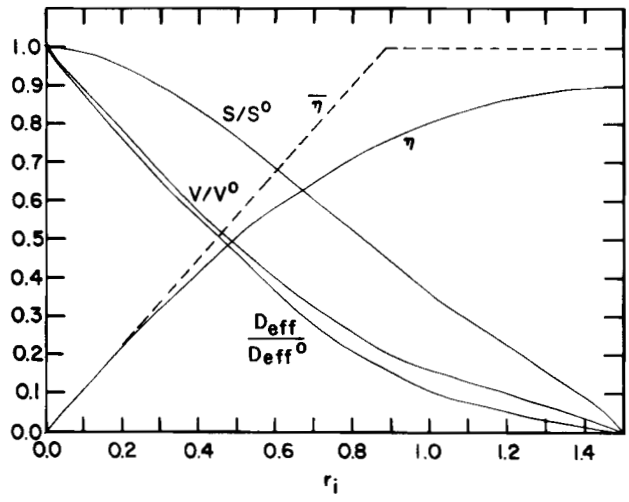

Figure 9. Normalized conversion, accessible surface area, volume, and effective diffusivity for Rayleigh distribution (a = 0), Z = 12, plotted vs. r_i.

tice with a Rayleigh original pore size distribution, for different values of the coordination number. Note that radius r_i and the cutoff radius in the Rayleigh distribution are made dimensionless with the characteristic length $1/\sqrt{\mu}$. As anticipated from Eq. 48, the conversion is consistently lower than the conversion obtained for the idealized porous medium. Conversion efficiencies are lower for lower values of the coordination number (compare Figure 7 to Figure 8, and Figure 9 to Figure 10), for smaller accessible fractions, and for original pore size distributions that contain a larger fraction of smaller pore sizes (compare Figures 7 and 8 to Figures 9 and 10). Conversion at early stages of the process is close to the conversion in the idealized porous medium, due to a smaller fraction of nonaccessible pores at early times ($X^A(1 - X_i) \simeq 1 - X_i$). The discrepancy is progressively pronounced at later stages in the reaction process. The effect of Biot number, absent from η vs. r_i plots, is introduced when conversion efficiency is plotted vs. time, made dimensionless by normalizing with the characteristic time K/D_e, (Figure 11). We notice a continuously increasing deviation from the idealized network predictions for increasing values of the Biot number.

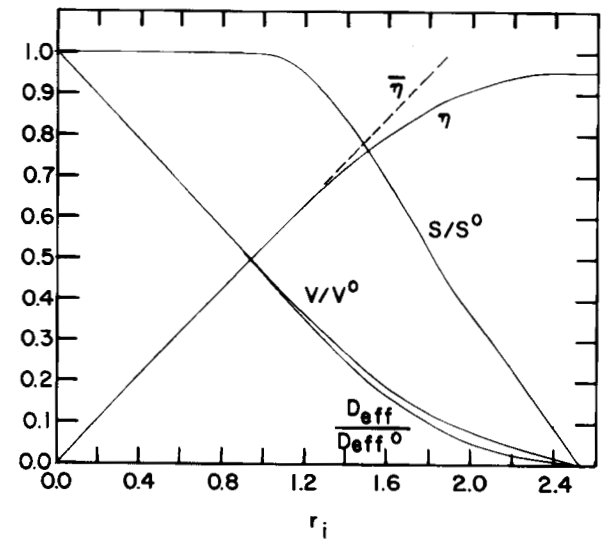

Figure 10. Normalized conversion, accessible surface area, volume, and effective diffusivity for Rayleigh distribution (a = 1), Z = 12, plotted vs. r_i.

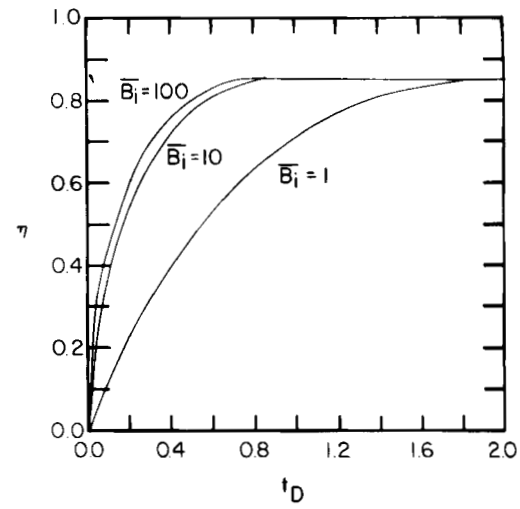

Figure 11. Normalized conversion for Rayleigh distribution vs. time.

Surface Area and Volume

Quantities related to the fraction and size distribution of open, accessible pores are calculated based on knowledge of the actual pore size distribution, f_a. Open, accessible pores have original pore size $r_o > r_i$. In view of Eq. 27 the accessible surface area for parallel-plate pore geometry becomes

$$S(r_i) \propto X^A(1 - X_i)\int_0^\infty f_a(r,r_i)dr \tag{49}$$

thus, the ratio of accessible surface area to original surface area S^o is

$$\frac{S(r_i)}{S^o} = X^A(1 - X_i) \tag{50}$$

A similar expression can readily be derived for the accessible volume

$$\frac{V(r_i)}{V^o} = \frac{X^A(1 - X_i)}{(1 - X_i)} \frac{\int_0^\infty rf(r + r_i)dr}{\int_0^\infty rf(r)dr} \tag{51}$$

Schematic illustrations of the evolution of the accessible surface area and volume for a Rayleigh distribution as a function of the coordination number are shown in Figures 7–10. A higher rate of decrease is shown to result for lower values of Z. As expected, the accessible surface area and volume reduce to zero as closure time is approached. It should be noted that for the parallel-plate pore model, S/S^o remains constant in the absence of blocked pores (Figures 9, 10).

Effective Diffusivity

In calculating effective diffusivity we assume for simplicity that the conductance of a single pore is related to its size by the relationship $g \propto r$. Other functional forms, including Knudsen diffusion, can also be considered, as desired. Following Stinchcombe (1974), the effective conductance g_{eff} of a Bethe tree lattice at high values of Z is obtained from the equation

$$g_{eff} \propto - Zx \tag{52}$$

where x is the root of the integral equation

$$\int_0^\infty G(g)\left[\frac{g(Z - 1)}{g - (Z - 1)x} - 1\right]dg = 0 \tag{53}$$

For a network consisting of a set of blocked pores of fraction X_b, and a set of open pores of fraction $1 - X_b$, the conductance distribution $G(g)$ is given by the equation (Heiba et al., 1982)

$$G(g) = X_b\delta(g) + (1 - X_b)\,\mathcal{G}(g) \tag{54}$$

where $\mathcal{G}(g)$ is the conductance distribution function of the open pores. The latter is calculated as a function of the pore size distributions f, f_{na}

$$\mathcal{G}(g)dg = \left[\frac{X^A(1 - X_i)f(r + r_i)}{(1 - X_b)(1 - X_i)} + \frac{1 - X_b - X^A(1 - X_i)}{(1 - X_b)} f_{na}(r,r_i)\right]dr \tag{55}$$

Substitution of Eq. 55 in Eqs. 54 and 53 results in an integral equation for x, the solution of which is obtained by standard numerical techniques. The evolution of the effective diffusivity normalized with respect to its value at the beginning of the process is obtained from the relationship

$$\frac{D_{\text{eff}}(r_i)}{D_{\text{eff}}^{\,o}} = \frac{g_{\text{eff}}(r_i)}{g_{\text{eff}}^{\,o}} \tag{56}$$

Numerical results for the normalized effective diffusivity are shown in Figures 7–10 for various coordination numbers and original pore size distributions, and in Figure 12 for various values of the Biot number. A monotonic decrease of the effective diffusion coefficient is noted as the reaction extent increases. The effect of the pore structure parameters and the Biot number, based on product layer diffusion, is similar to the effect on conversion. Near pore closure time the effective diffusion coefficient rapidly approaches a negligibly small value, as intuitively expected.

Global Formulation

The above results, valid for a differential element under kinetic control, are also globally valid if the porous medium is globally under kinetic control. If the latter restriction is not applicable we can incorporate the previous analysis into a global mathematical model as follows.

When the process is not kinetically controlled the local concentration C_A is a function of time. From the definition of the parametrization function, Eq. 10, we have

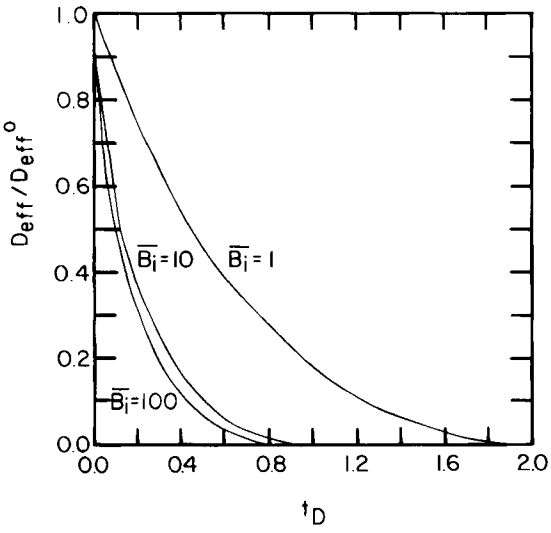

Figure 12. Normalized effective diffusivity for Rayleigh distribution vs. time.

$$\lambda C_A dt = \left[\frac{d}{dr_i}\int_0^{r_i} G_s(r;r_i)dr\right]dr_i \tag{57}$$

where λ is a kinetic constant. Following integration of Eq. 57 we obtain in functional form

$$r_i = r_i\left(\int_0^t C_A dt\right) \tag{58}$$

Therefore, the effective diffusivity D_{eff} is a unique function of the variable $\int_0^t C_A dt$ (compare to Eq. 56)

$$D_{\text{eff}} = D_{\text{eff}}\left(\int_0^t C_A dt\right) \tag{59}$$

The differential conversion dR is a measure of the reaction rate for gas A. Using Eqs. 44 and 57 we write in general notation

$$dR = U\left[\int_0^t C_A dt\right] C_A dt \tag{60}$$

where the reaction rate function U can readily be calculated in terms of the accessibility function.

We now insert expressions 59 and 60 into a global differential mass balance. Following the quasisteady-state assumption we get in terms of global coordinates

$$\nabla\left(D_{\text{eff}}\left(\int_0^t C_A dt\right)\nabla C_A\right) = U\left(\int_0^t C_A dt\right) C_A \tag{61}$$

The integration of Eq. 61 can be performed most conveniently by using the representation

$$\nabla \cdot (D_{\text{eff}}(u)\nabla C_A) = U(u)C_A \tag{62a}$$

$$\frac{\partial u}{\partial t} = C_A \tag{62b}$$

Those expressions allow for the effective diffusivity to vary during the course of the reaction in a manner that reflects the topology and geometry of the porous medium. Numerical solution techniques for Eq. 62 have been devised in the past for arbitrary porous particle geometries. In the case of slab particle geometries we obtain

$$\frac{\partial}{\partial z}\left(D_{\text{eff}}(u)\frac{\partial C_A}{\partial z}\right) = U(u)C_A \tag{63a}$$

$$\frac{\partial u}{\partial t} = C_A \tag{63b}$$

Analytical solutions in the limit of global diffusion control for the above equations have been developed by Yortsos and Shankar (1984).

DISCUSSION

In this paper a mathematical formulation for noncatalytic gas-solid reaction processes that lead to pore closure has been presented. Central in the theoretical development is the representation of the porous medium in terms of network approximation. Using concepts from percolation theory, a theoretical framework for the determination of the evolution in time of process quantities, such as conversion, accessible surface area, and effective diffusivity, has been constructed. The analysis is based on the hypothesis of kinetic control in a local, representative element of the porous medium. For reaction conditions such that the porous medium is globally in the kinetic control regime, the expressions ob-

tained represent the global behavior of the process. When this constraint is not satisfied, a suitable global model was developed by relating local conversion and local diffusion coefficient to the state of the local model. The network formulation presented here allows for direct calculation of the effective diffusivity, which was found to decrease with an increase in process time. It should be pointed out that most of the existing mathematical models postulate either a constant diffusion coefficient or some a priori relation between diffusion coefficient and porosity, a limitation that is expected to result in additional overestimation of conversion efficiency.

The theory was developed under certain simplifying approximations, such as Bethe lattices, parallel-plate pores, and assignment of negligible volume to sites, in order to obtain computationally simple expressions. Relaxation of these approximations can easily be implemented for a particular system of interest at the cost of more elaborate calculations. We anticipate that the theory can be extended directly to apply to closely related processes, such as catalyst deactivation and deep-bed filtration. On the other hand, the above formulation cannot be applied in its present form to gasification type reactions when the radii of the pores increase with process time. In these processes additional effects, such as pore overlapping, may not be amenable to a simple mathematical treatment using percolation theory concepts.

It was shown that neglecting topologically important quantities such as the nonaccessible fraction of open pores results in lower estimates of pore closure time and higher estimates of conversion. The discrepancy of the above predictions to those obtained by parallel-pore models of constant radius was found to be increasing with an increase in the Biot number, based on product layer diffusion, an increase in process time, a decrease in the coordination number, and an increase in the standard deviation of the pore size distribution. This comparison was made for the purpose of illustrating the effects of topology on the reaction performance. No comparison was attempted with the distributed pore size model of Christman and Edgar (1983), or the random pore models of Gavalas (1980) and Batia and Perlmutter (1980). However, since the latter works do not address the question of network accessibility, we anticipate a discrepancy that would be larger as the coordination number decreases.

The theory presented here can be used to model the performance of a noncatalytic gas-solid reaction process leading to pore closure, given the true pore size distribution, the coordination number of the porous medium, and the Biot number. Conversely, the expressions derived can be utilized to estimate process parameters, such as the kinetic constant or the diffusion coefficient in the product layer, an a priori estimate of which is not readily available.

NOTATION

b = stoichiometric coefficient, dimensionless
Bi = Biot number, dimensionless
C_A = gas concentration, mol/L^3
d = stoichiometric coefficient, dimensionless
D = dimensionality, dimensionless
D_e = product layer diffusivity, L^2/T
D_{eff} = effective diffusivity, L^2/T
f = distribution function, L^{-1}
g = conductance, L^2/T
K = reaction constant, L/T
M = molecular weight, M/mol
p_c = percolation threshold, dimensionless
r = pore size, L
r_f = reaction interface, L
R = conversion, M/L^3
s = geometry index
S = surface area, L^2
t = time, T
V = molar volume, L^3/mol
X = pore fraction, dimensionless
Z = coordination number, dimensionless

Greek Letters

α = parameter, dimensionless
ϵ = porosity, dimensionless
η = normalized conversion, dimensionless
ϱ = density, M/L^3

Subscripts

a = accessible
b = blocked pores
eff = effective
i = parametrization index
na = nonaccessible
o = original
p = pore closure

Superscripts

A = accessibility
o = original

APPENDIX

We consider the population balance equation

$$\frac{\partial}{\partial r_i}[X_a f_a] - \frac{\partial}{\partial r}[X_a f_a] = -\frac{dX_{na}}{dr_i} f_a \tag{A1}$$

and introduce the coordinate transformation $y = r + r_i$, $x = r_i$. By denoting $A = X_a$, $B = X_{na}$, Eq. A1 becomes

$$\frac{\partial}{\partial x}[A f_a] = -\frac{dB}{dr_i} f_a(y - x,x) \tag{A2}$$

which, if integrated with respect to x yields

$$A(x) f_a(y - x,x) + \int_0^x \frac{dB}{dx'} f_a(y - x',x')dx' = f(y) \tag{A3}$$

By denoting

$$L(y,x) = \frac{f_a(y - x,x)}{f(y)} \tag{A4}$$

Eq. A3 is

$$A(x)\, L(y,x) + \int_0^x \frac{dB}{dx'} L(y,x')dx' = 1 \tag{A5}$$

By differentiating Eq. A5 with respect to y and denoting

$$I(y,x) = \frac{\partial L}{\partial y} \tag{A6}$$

Eq. A5 yields

$$A(x) = -\int_0^x \frac{dB}{dx'} \frac{I(y,x')}{I(y,x)} dx' \tag{A7}$$

which implies

$$I(y,x') = \mathrm{F}(x,x')\, I(y,x) \tag{A8}$$

where F is arbitrary. Integration of Eq. A8 with respect to y and use of Eq A6 yields

$$L(y,x') = F(x,x')\ L(y,x) + H(x,x') \quad \text{(A9)}$$

Evaluating Eq. A9 at $x' = 0$ and making use of Eq. A4 and the condition $f_a(y,0) = f(y)$ we obtain

$$F(x,0)\ L(y,x) + H(x,0) = 1 \quad \text{(A10)}$$

which further implies

$$L(y,x) = \theta(x) \quad \text{(A11)}$$

Thus, by Eq. A4 we finally recover

$$f_a(y - x,x) = f(y)\ \theta(x) \quad \text{(A12)}$$

or, in terms of the original variables

$$f_a(r,r_i) = f(r + r_i)\ \theta\ (r_i) \quad \text{(A13)}$$

as postulated in the main text.

A similar approach also holds for other than parallel-plate pore geometries involving general functional forms $G_s(r;r_0)$.

LITERATURE CITED

Bhatia, S. K., and D. D. Perlmutter, "A Random Porel Model for Fluid-Solid Reactions. 1: Isothermal, Kinetic Control," *AIChE J.*, **26**, 376 (1980).

Broadbent, S. R., and T. M. Hammersley, "Percolation Processes, Crystals and Mazes," **Proc. Camb. Phil. Soc.**, **53**, 629 (1957).

Butt, J. B., *Adv. Chem. Ser.*, **109**, 259 (1972).

Christman, P. G., and T. F. Edgar, "Distributed Pore-Size Model for Sulfation of Limestone," *AIChE J.*, **29**, 388 (1983).

Fisher, M. E., and J. W. Essam, "Some Cluster Size and Percolation Problems," *J. Math. Phys.*, **2**(4), 609 (1961).

Garza-Garza, O., and M. P. Dudukovic, "Some Observations on Gas-Solid Noncatalytic Reactions with Structural Changes," *Chem. Eng. Sci.*, **36**, 1,257 (1981).

Gavalas, G. R., "A Random Capillary Model with Application to Char Gasification at Chemically Controlled Rates," *AIChE J.*, **26**, 577 (1980).

Gruesbeck, C., and R. E. Collins, "Entrainment and Deposition of Fine Particles in Porous Media," *Soc. Pet. Eng. J.*, **22**, 847 (1982).

Heiba, A. A., et al., "Percolation Theory of Two-Phase Relative Permeability," *SPE Paper 11,015*, 57th Ann. Meet., New Orleans (Sept., 1982).

Heiba, A. A., H. T. Davis, and L. E. Scriven, "Effect of Wettability on Two-Phase Relative Permeabilities and Capillary Pressures," *SPE Paper 12,172*, 58th Ann. Meet., San Francisco (Oct., 1983).

———, "Statistical Network Theory of Three-Phase Relative Permeabilities," *SPE Paper 12,690*, SPE/DOE 4th Symp. on Enhanced Oil Recovery, Tulsa (Apr., 1984).

Kirkpatrick, S., "Percolation and Conduction," *Rev. Mod. Phys.*, **45**, (4), 574 (1973).

Larson, R. G., H. T. Davis, and L. E. Scriven, "Percolation Theory of Two-Phase Flow in Porous Media," *Chem. Eng. Sci.*, **36**, 57 (1981a).

———, "Displacement of Residual Nonwetting Fluid from Porous Media," *Chem. Eng. Sci.*, **36**, 75 (1981b).

Mohanty, K. K., A. B. Ottino, and H. T. Davis, "Reaction and Transport in Disordered Composite Media: Introduction of Percolation Concepts," *Chem. Eng. Sci.*, **37**, 905 (1982).

Ramachandran, P. A., and L. K. Doraiswamy, "Modeling of Noncatalytic Gas-Solid Rections," *AIChE J.*, **28**, 881 (1982).

Ramachandran, P. A., and J. M. Smith, "A Single-Pore Model for Gas-Solid Noncatalytic Reactions," *AIChE J.*, **23**, 353 (1977).

Shankar, K., and Y. C. Yortsos, "Asymptotic Analysis of Single-Pore Gas-Solid Reactions," *Chem. Eng. Sci.*, **38**, 1,159 (1983).

Shante, V. K., and S. Kirkpatrick, "An Introduction to Percolation Theory," *Adv. Phys.*, **20**, 325 (1971).

Sharma, M. M., and Y. C. Yortsos, "Transport of Particulate Suspensions in Porous Media," submitted (1984).

Stauffer, D., "Scaling Theory of Percolating Clusters," *Phys. Report*, **54**, 1 (1979).

Stinchcombe, R. B., "Conductivity and Spin-Wave Stiffness in Disordered Systems—An Exactly Soluble Model," *J. Phys. C.: Solid State Phys.*, **7**, 179 (1974).

Szekely, J., and J. W. Evans, "A Structural Model for Gas-Solid Reactions with a Moving Boundary," *Chem. Eng. Sci.*, **25**, 1,091 (1970).

Tien, C., and A. C. Payatakes, "Advances in Deep Bed Filtration," *AIChE J.*, **25**, 737 (1979).

Yortsos, Y. C., and K. Shankar, "Asymptotic Analysis of Pore Closure Reactions," *Ind. Eng. Chem. Fund.*, **23**, 132 (1984).

Manuscript received July 3, 1984, and revision received Nov. 27, 1984.